

# *Supporting Information*

## Dynamics of Hydroxide-Ion-driven Reversible Autocatalytic Networks

Emese Lantos,<sup>a</sup> Gergő Mótyán,<sup>b</sup> Éva Frank,<sup>b</sup> Rienk Eelkema,<sup>c</sup> Jan van Esch,<sup>c</sup>  
Dezső Horváth,<sup>d</sup> and Ágota Tóth\*<sup>a</sup>

<sup>a</sup> *Department of Physical Chemistry and Materials Science, University of Szeged,  
Rerrich Béla tér 1., Szeged, H-6720, Hungary. E-mail: atoth@chem.u-szeged.hu*

<sup>b</sup> *Department of Organic Chemistry, University of Szeged, Dóm tér 8., Szeged, H-6720, Hungary.*

<sup>c</sup> *Department of Chemical Engineering, Delft University of Technology, Van der Maasweg 9., 2629 HZ Delft, Netherlands.*

<sup>d</sup> *Department of Applied and Environmental Chemistry, University of Szeged, Rerrich Béla tér 1., Szeged, H-6720, Hungary.*

June 23, 2023

## Contents

<b>1</b>	<b>Experimental section: Calibration</b>	<b>S2</b>
<b>2</b>	<b>Supporting figures</b>	<b>S2</b>
<b>3</b>	<b>Modeling</b>	<b>S5</b>
3.1	Eight-variable model . . . . .	S5
3.2	Two-variable model . . . . .	S5
3.3	Optimization of rate coefficients . . . . .	S6

# 1 Experimental section: Calibration

To be sure, that despite of adding absolute ethanol to the system, we measured appropriate pH values we carried out control experiments. For this purpose we prepared solutions with different pH covering the pH = 1-12 range using 10-90V/V% ethanol-water solvent ratio and recorded the potential. Later, we compared the values recorded in the buffer solutions used for the two-point calibration and prepared with deionized water.

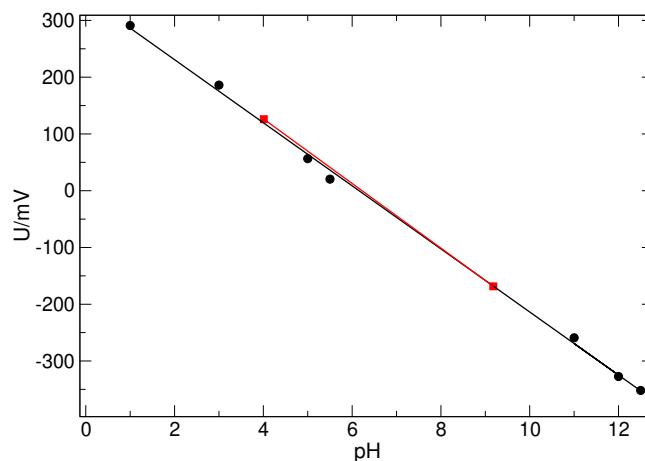


Figure S1: The comparison of the potential measured at different pH in case of deionized water and 10–90% ethanol–deionized water as solvent. ■ : buffer solutions using pure deionized water; ● : control measurements with 10–90 V/V% water-ethanol compound at different pH. It is observable that there is no difference between the solvents in the view of the slope of the fitted line.

## 2 Supporting figures

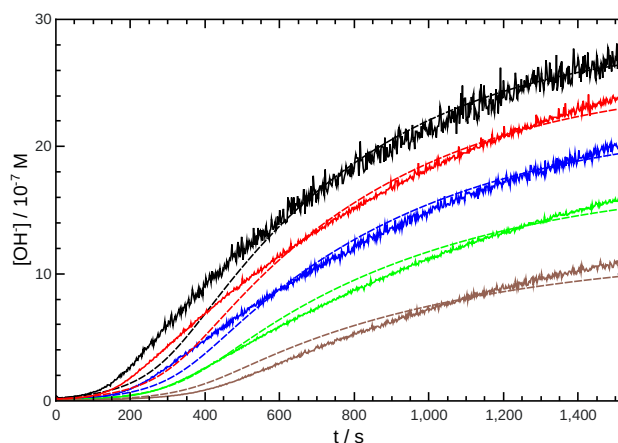


Figure S2: Time evolution of the  $[\text{OH}^-]$  for imine "B" with 1 mM initial reactant concentration. Initial pH decreases from black to orange: 6.34 (black), 6.19 (red), 6.04 (blue), 5.88 (green), 5.62 (brown). Experimental measurements are shown with solid lines and the simulated curves with dashed lines.

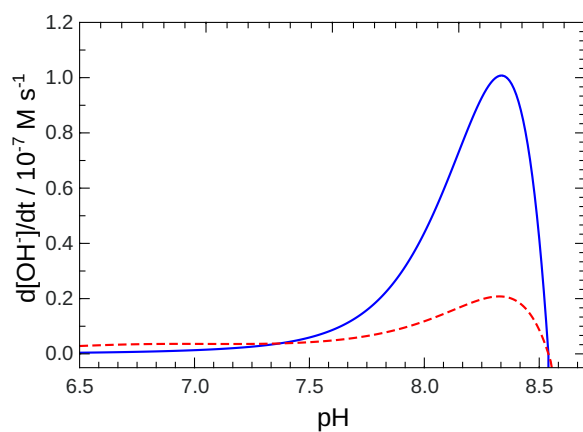


Figure S3: Rate of  $\text{OH}^-$  production as a function of pH for reactant mixture with  $S_T = 1 \text{ mM}$ ,  $B_T = O_{xT} = 0 \text{ mM}$  (blue solid line) and for composition corresponding to 55 % conversion with  $S_T = 0.446 \text{ mM}$ ,  $B_T = O_{xT} = 0.554 \text{ mM}$  (red dashed line).

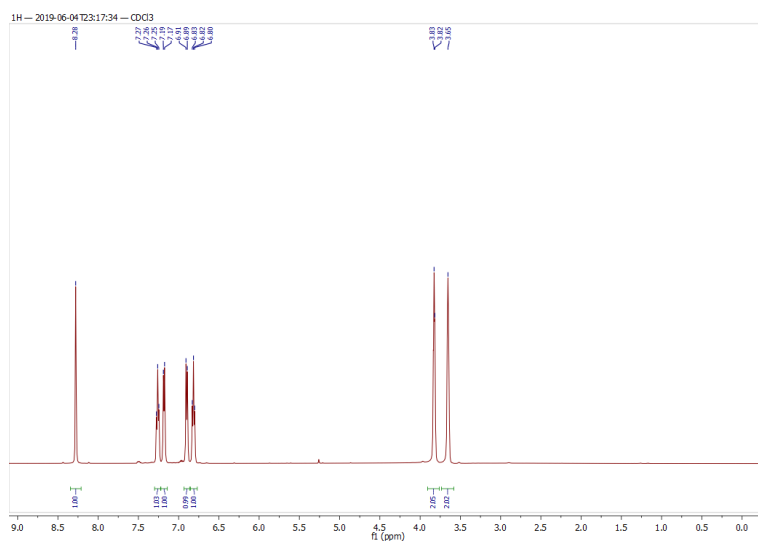


Figure S4: The  $^1\text{H}$  NMR spectrum of the synthesized imine "A" (500 MHz,  $\text{CDCl}_3$ ).

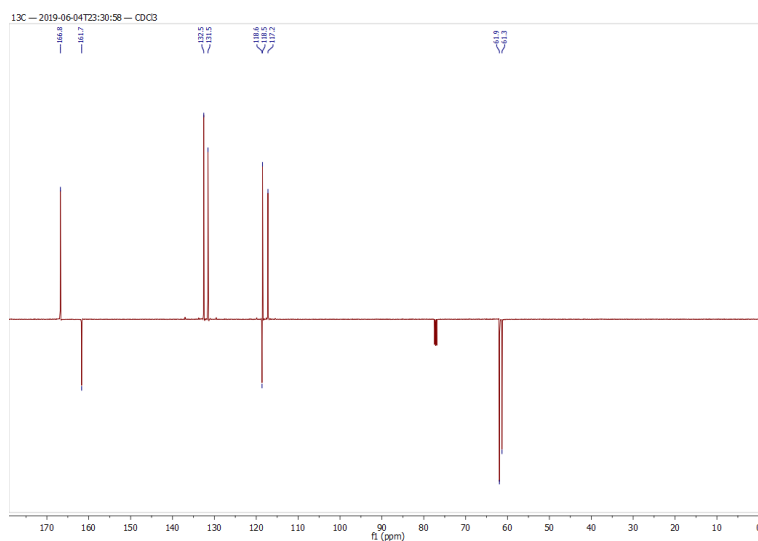


Figure S5: The  $^{13}\text{C}$  NMR spectrum of the synthesized imine "A" (125 MHz,  $\text{CDCl}_3$ ).

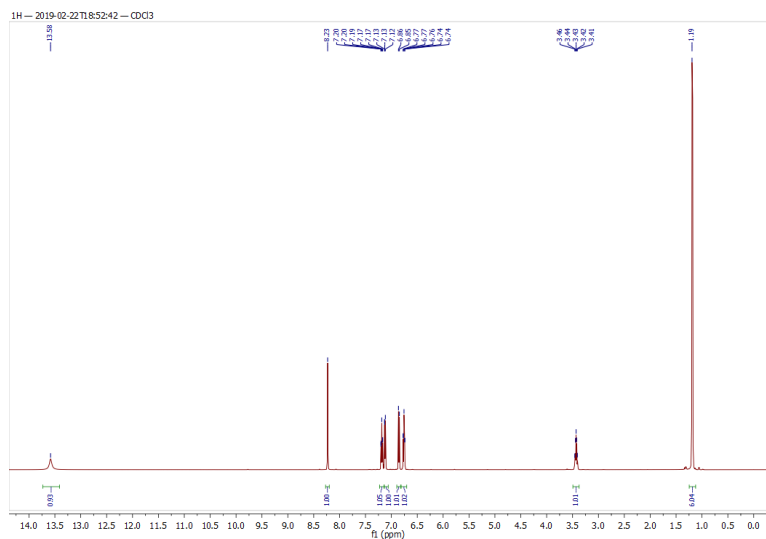


Figure S6: The  $^1\text{H}$  NMR spectrum of the synthesized imine "B" (500 MHz,  $\text{CDCl}_3$ ).

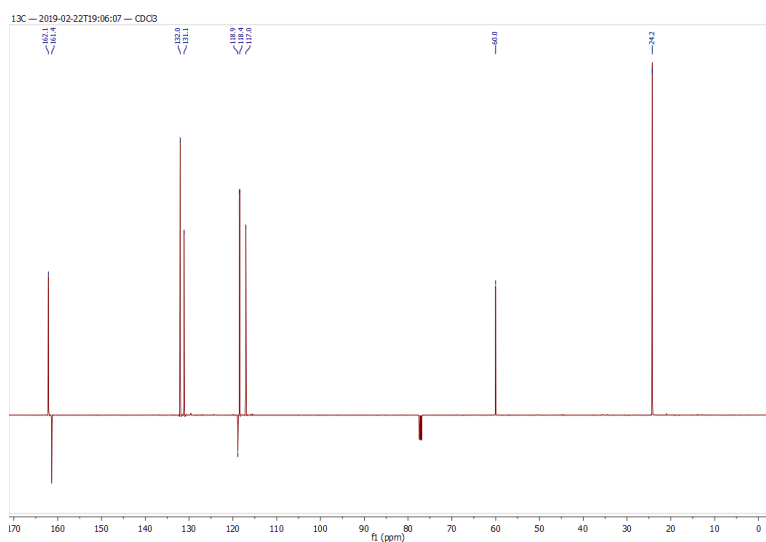


Figure S7: The  $^{13}\text{C}$  NMR spectrum of the synthesized imine "B" (125 MHz,  $\text{CDCl}_3$ ).

## 3 Modeling

### 3.1 Eight-variable model

The differential equations for each species based on the governing equations of the 8-variable-model presented in the main text in Eqns. (2)–(8) are the following:

$$\frac{d[S]}{dt} = -k_1[S] + k_{-1}[\text{SH}^+][\text{OH}^-] - k_6[S][\text{OH}^-] \quad (\text{S1})$$

$$\frac{d[\text{SH}^+]}{dt} = k_1[S] - k_{-1}[\text{SH}^+][\text{OH}^-] - k_2[\text{SH}^+][\text{OH}^-] - k_5[\text{SH}^+] \quad (\text{S2})$$

$$\frac{d[B]}{dt} = k_2[\text{SH}^+][\text{OH}^-] - k_3[B] + k_{-3}[\text{BH}^+][\text{OH}^-] + k_6[S][\text{OH}^-] \quad (\text{S3})$$

$$\frac{d[\text{BH}^+]}{dt} = k_3[B] - k_{-3}[\text{BH}^+][\text{OH}^-] + k_5[\text{SH}^+] \quad (\text{S4})$$

$$\frac{d[\text{Ox}]}{dt} = k_2[\text{SH}^+][\text{OH}^-] + k_5[\text{SH}^+] + k_7[\text{Ox}^-] - k_{-7}[\text{Ox}][\text{OH}^-] \quad (\text{S5})$$

$$\frac{d[\text{Ox}^-]}{dt} = k_6[S][\text{OH}^-] - k_7[\text{Ox}^-] + k_{-7}[\text{Ox}][\text{OH}^-] \quad (\text{S6})$$

$$\frac{d[\text{H}^+]}{dt} = k_4 - k_{-4}[\text{H}^+][\text{OH}^-] \quad (\text{S7})$$

$$\begin{aligned} \frac{d[\text{OH}^-]}{dt} = & k_1[S] - k_{-1}[\text{SH}^+][\text{OH}^-] - k_2[\text{SH}^+][\text{OH}^-] + k_3[B] - k_{-3}[\text{BH}^+][\text{OH}^-] + \\ & + k_4 - k_{-4}[\text{H}^+][\text{OH}^-] - k_6[S][\text{OH}^-] + k_7[\text{Ox}^-] - k_{-7}[\text{Ox}][\text{OH}^-] \end{aligned} \quad (\text{S8})$$

The autonomous ordinary differential equations given by Eqns. (S1)–(S8) that describe the temporal evolution of concentrations have been solved by *Copasi*. For the stability analysis of the steady states and their continuation in the parameter space, we have used the *AUTO* bifurcation program within the *XPPAUT* package.

### 3.2 Two-variable model

Since the total imine concentration is  $S_T = [S] + [\text{SH}^+]$ , its temporal change is

$$\frac{dS_T}{dt} = \frac{d[S]}{dt} + \frac{d[\text{SH}^+]}{dt} = -k_2[\text{SH}^+][\text{OH}^-] - k_5[\text{SH}^+] - k_6[S][\text{OH}^-]. \quad (\text{S9})$$

Using the equilibrium constant for Eqn. (2) as  $K_1 = \frac{[\text{SH}^+][\text{OH}^-]}{[S]}$  with substituting in  $[S] = S_T - [\text{SH}^+]$  or  $[\text{SH}^+] = S_T - [S]$  leads to

$$[\text{SH}^+] = S_T \frac{K_1}{K_1 + [\text{OH}^-]} \quad \text{and} \quad [S] = S_T \frac{[\text{OH}^-]}{K_1 + [\text{OH}^-]}, \quad (\text{S10})$$

from which

$$\frac{dS_T}{dt} = -\frac{S_T}{K_1 + [\text{OH}^-]} (K_1 k_5 + K_1 k_2 [\text{OH}^-] + k_6 [\text{OH}^-]^2) = -S_T \frac{K_1 k_2 [\text{OH}^-] + K_1 k_5 + k_6 [\text{OH}^-]^2}{K_1 + [\text{OH}^-]}. \quad (\text{S11})$$

For the change in the total amine concentration, we can write

$$\frac{dB_T}{dt} = \frac{d[B]}{dt} + \frac{d[\text{BH}^+]}{dt} = k_2[\text{SH}^+][\text{OH}^-] + k_5[\text{SH}^+] + k_6[S][\text{OH}^-] = -\frac{dS_T}{dt} \quad (\text{S12})$$

and similarly for the salicylaldehyde with  $Ox_T = [Ox] + [Ox^-]$  we obtain  $\frac{dOx_T}{dt} = -\frac{dS_T}{dt}$  with  $[Ox^-] = Ox_T \frac{[OH^-]}{K_7 + [OH^-]}$ . Therefore,

$$B_T = Ox_T = S_{T,0} - S_T \quad (S13)$$

where  $S_{T,0}$  is the initial total concentration of the imine. The concentration of hydrogen ion can always be expressed from the concentration of hydroxide ion, therefore, besides Eqn. (S11), only the temporal change in the hydroxide ion concentration (Eqn. (S8)) has to be considered. From Eqns. (S1)–(S7), the temporal change in the hydroxide ion concentration becomes

$$\frac{d[OH^-]}{dt} = \frac{d[SH^+]}{dt} + \frac{d[BH^+]}{dt} + \frac{d[H^+]}{dt} - \frac{d[Ox^-]}{dt}. \quad (S14)$$

From Eqn. (S10), we find

$$\frac{d[SH^+]}{dt} = \frac{d}{dt} \left( S_T \frac{K_1}{K_1 + [OH^-]} \right) = \frac{K_1}{K_1 + [OH^-]} \frac{dS_T}{dt} - \frac{K_1 S_T}{(K_1 + [OH^-])^2} \frac{d[OH^-]}{dt}. \quad (S15)$$

Similarly for the amine,

$$\frac{d[BH^+]}{dt} = \frac{d}{dt} \left( B_T \frac{K_3}{K_3 + [OH^-]} \right) = -\frac{K_3}{K_3 + [OH^-]} \frac{dS_T}{dt} - \frac{K_3(S_{T,0} - S_T)}{(K_3 + [OH^-])^2} \frac{d[OH^-]}{dt}, \quad (S16)$$

for the hydrogen ion,

$$\frac{d[H^+]}{dt} = \frac{d}{dt} \frac{K_w}{[OH^-]} = -\frac{K_w}{[OH^-]^2} \frac{d[OH^-]}{dt}, \quad (S17)$$

and for the deprotonated form of the aldehyde

$$\frac{d[Ox^-]}{dt} = \frac{d}{dt} \left( \frac{Ox_T [OH^-]}{K_7 + [OH^-]} \right) = -\frac{[OH^-]}{K_7 + [OH^-]} \frac{dS_T}{dt} + \frac{K_7(S_{T,0} - S_T)}{(K_7 + [OH^-])^2} \frac{d[OH^-]}{dt}, \quad (S18)$$

yielding for Eqn. (S14)

$$\frac{d[OH^-]}{dt} = \frac{\left( \frac{(K_1 - K_3)[OH^-]}{(K_1 + [OH^-])(K_3 + [OH^-])} + \frac{[OH^-]}{K_7 + [OH^-]} \right) \frac{dS_T}{dt}}{1 + \frac{K_1 S_T}{(K_1 + [OH^-])^2} + \frac{K_3(S_{T,0} - S_T)}{(K_3 + [OH^-])^2} + \frac{K_w}{[OH^-]^2} + \frac{K_7(S_{T,0} - S_T)}{(K_7 + [OH^-])^2}}. \quad (S19)$$

### 3.3 Optimization of rate coefficients

Copasi software package is also used for the parameter adjustment by fitting the calculated  $OH^-$ -concentration–time curves to all the experimentally measured data sets simultaneously using nonlinear least-squares method with the Levenberg-Marquardt optimization for the minimalization. For imine "A" from nine different experiments 4203 points and from imine "B" from five different experiments 3820 points were used to optimize the parameters. In the course of fitting the experimental curves, we have added an extra parameter  $\xi$ , which includes the uncertainty coming from the volume measurements of the viscous Schiff-base in the sample. The upper limit of this value was set to 1.5 and the lower to 0.3 for the estimation. In case of reversible steps the backward processes have been assumed to be diffusion controlled with fixed value of 2 or  $5 \times 10^8 \text{ dm}^3 \text{ mol}^{-1} \text{ s}^{-1}$ . Literature value of  $1 \times 10^{-14} \text{ dm}^3 \text{ mol}^{-1} \text{ s}^{-1}$  has been used for  $K_w$ .